POLITECNICO DI TORINO
Repository ISTITUZIONALE

Scar states in deconfined Z2 lattice gauge theories

Original
Scar states in deconfined Z2 lattice gauge theories / Aramthottil, A.S., Bhattacharya, U., González-Cuadra, D., Lewenstein, M., Barbiero, L., Zakrzewski, J.. - In: PHYSICAL REVIEW. B. - ISSN 2469-9950. - ELETTRONICO. - 106:4(2022). [10.1103/PhysRevB.106.L041101]

Availability:
This version is available at: 11583/2969418 since: 2022-09-23T12:05:04Z

Publisher:
American Physical Society

Published
DOI:10.1103/PhysRevB.106.L041101

Terms of use:

This article is made available under terms and conditions as specified in the corresponding bibliographic description in the repository

Publisher copyright

(Article begins on next page)

30 October 2026

Letter

Scar states in deconfined $\mathbb{Z}_2$ lattice gauge theories

Adith Sai Aramthottil,[1] Utso Bhattacharya,[2] Daniel González-Cuadra,[2,3,4] Maciej Lewenstein,[2,5] Luca Barbiero,[6,2] and Jakub Zakrzewski[1,7]

[1]*Instytut Fizyki Teoretycznej, Uniwersytet Jagielloński, Łojasiewicza 11, PL-30-348 Kraków, Poland*
[2]*ICFO-Institut de Ciències Fotòniques, The Barcelona Institute of Science and Technology, Avenida Carl Friedrich Gauss 3, E-08860 Castelldefels (Barcelona), Spain*
[3]*Institute for Theoretical Physics, University of Innsbruck, A-6020 Innsbruck, Austria*
[4]*Institute for Quantum Optics and Quantum Information of the Austrian Academy of Sciences, A-6020 Innsbruck, Austria*
[5]*ICREA, Passeig Lluis Companys 23, E-08010 Barcelona, Spain*
[6]*Institute for Condensed Matter Physics and Complex Systems, DISAT, Politecnico di Torino, I-10129 Torino, Italy*
[7]*Mark Kac Complex Systems Research Center, Uniwersytet Jagielloński, Kraków PL-30-348, Poland*

(Received 1 February 2022; revised 17 March 2022; accepted 22 June 2022; published 1 July 2022)

The weak ergodicity breaking induced by quantum many-body scars (QMBSs) represents an intriguing concept that has received great attention in recent years due to its relation to unusual nonequilibrium behavior. Here, we reveal that this phenomenon can occur in a particular regime of a lattice gauge theory, where QMBSs emerge due to the presence of an extensive number of local constraints. In particular, by analyzing the gauged Kitaev model, we provide an example where QMBSs appear in a regime where charges are deconfined. By means of both numerical and analytical approaches, we find a variety of scarred states far away from the regime where the model is integrable. The presence of these states is revealed both by tracing them directly from the analytically reachable limit, as well as by quantum quenches showing persistent oscillations for specific initial states.

DOI: 10.1103/PhysRevB.106.L041101

Introduction. The thermalization properties of isolated quantum systems are currently under intensive investigation in different areas of modern quantum physics [1–4]. In this context, huge attention has been recently devoted towards the study of a large variety of Hamiltonians where the ergodicity is weakly broken [5–24]. In particular, in such models quenches from carefully designed initial states reveal persistent many-body revivals that apparently contradict ergodicity [5,25]. The reason for such an absence of thermalization turns out to be the presence of specific eigenstates called quantum many-body scars (QMBSs) characterized, in particular, by a subvolume entanglement law [6–14,21,24,26]. It is worth noting that similar regular states have been previously identified [27] for chaotic quantum billiards in relation to semiclassical periodic orbit quantization [28,29]. Moreover, the concept of scarred symmetry, closely related to QMBSs, has been introduced in studies of a hydrogen atom in a strong magnetic field [30].

With the advent of a new generation of cold-atom quantum simulators [31–35], the weak ergodicity breaking manifested by QMBSs has been experimentally detected in constrained spin [5] and bosonic [36] models. Crucially, both realizations can be viewed as lattice gauge theories (LGTs) where the energy constraints are induced by the Gauss law fixing the relation between gauge and charge variables. Motivated by the recent progress achieved in the last years in implementing LGTs in quantum simulators [37–42], an impressive theoretical effort has been devoted towards a better understanding of simple gauge-invariant theories [17,18,43–57]. In this direction, the connection between Gauss law and QMBSs has recently gained attention both in $U(1)$ [16,58] and $\mathbb{Z}_2$ [13] LGTs. Here, indeed, the weak ergodicity breaking associated with the slow oscillatory dynamics can be interpreted as a *string inversion* phenomenon. Crucially, it has to be underlined that all LGTs, where QMBSs have been identified, are characterized by charge confinement. This regime implies that only particle-antiparticle bound states exist and therefore charges can be observed in composite structures only. These effective pairs, together with an emergent new symmetry, generate the slowdown of quantum dynamics and have been shown to be intricately connected to the presence of QMBSs [59].

Thus it seems natural to wonder whether confinement is a prerequisite to observe QMBSs in LGTs. In this Letter, we tackle this question by investigating the recently introduced gauged one-dimensional (1D) Kitaev model [16,60,61], whose ground state displays a confined phase as well as a regime where charges are not bounded in pairs, thus describing a deconfined phase. We study its low-entanglement states and show that QMBSs are present in the ergodic deconfined phase and are absent in the ergodic confined regime of the model. Importantly, we are able to continuously track QMBSs down from the analytic prediction valid in the quasi-integrable regime and therefore provide their partial classification.

Model and observables. The Hamiltonian of the p-wave superconducting Kitaev chain minimally coupled to a $\mathbb{Z}_2$ gauge

 ©2022 American Physical Society

field introduced in Refs. [16,60,61] reads

$$H = -t\sum_j (c_j^\dagger - c_j)\sigma^z_{j+1/2}(c^\dagger_{j+1} + c_{j+1}) - \mu\sum_j\left(c_j^\dagger c_j - \frac{1}{2}\right) - h\sum_j \sigma^x_{j+1/2}. \quad (1)$$

Here, $c_j^\dagger$ (c_j) denotes the fermionic creation (annihilation) operator and t describes the tunneling and pair production/annihilation processes mediated by the $\mathbb{Z}_2$ gauge field $\sigma^z_{j+1/2}$ defined on the links between the nearest-neighbor sites. Fluctuations in the gauge field are induced by the electric field $\sigma^x_{j+1/2}$ of strength h and the number of fermions is fixed by the chemical potential μ. Here, $\sigma^i_{j+1/2}$ stands for standard Pauli matrices.

As required in LGTs, the model (1) is invariant under the local gauge transformation generated by the Gauss operator $G_j = \sigma^x_{j-1/2}(-1)^{n_j}\sigma^x_{j+1/2}$, where $[H, G_j] = 0$ and $[G_i, G_j] = 0$. Therefore, the physical states are those that satisfy the Gauss law, $G_j|\psi\rangle = \pm|\psi\rangle$, for all j sites [62].

The Hamiltonian (1) can be written in terms of gauge-invariant transformed Pauli operators:

$$X_{i+\frac{1}{2}} = \sigma^x_{i+\frac{1}{2}}, \quad (2)$$

$$Y_{i+\frac{1}{2}} = (c_i^\dagger - c_i)\sigma^y_{i+\frac{1}{2}}(c^\dagger_{i+1} + c_{i+1}), \quad (3)$$

$$Z_{i+\frac{1}{2}} = (c_i^\dagger - c_i)\sigma^z_{i+\frac{1}{2}}(c^\dagger_{i+1} + c_{i+1}). \quad (4)$$

Upon this transformation and with periodic boundary conditions, the gauged Kitaev model corresponds to the quantum Ising model with both transverse and longitudinal fields,

$$H = \sum_{i=1}^{L}\frac{\mu}{2}Z_iZ_{i+1} - tX_i - hZ_i. \quad (5)$$

Notice that the model is now defined on a dual lattice, where the index i corresponds to the links of the original model (1).

For $\mu > 0$, the phase diagram of the model (5), as shown in Fig. 1, is characterized by the presence of both an antiferromagnetic (AFM) order and a paramagnetic (PM) phase depending on parameters t and h [63]. The AFM phase turns out to be of great interest, since it supports domain-wall excitations associated with the antiferromagnetic order caused by the spontaneous breaking of the $\mathbb{Z}_2$ Ising and translational symmetries. In 1D these last two features imply domain-wall deconfinement. Therefore, in the gauged Kitaev Hamiltonian, (1), such an AFM order corresponds to charge deconfinement (CD), where fermions are free to expand without any string tension. On the other hand, the PM regime corresponds to a phase characterized by charge confinement (CC), where fermions appear only as bound pairs.

In the limit $t \ll \mu$ it is possible to perform a Schrieffer-Wolff transformation (in agreement with Ref. [60]; for a higher-order expansion, see Ref. [64]), with

$$S = \frac{-it}{2\mu}\sum_j\left\{\left(\frac{1+Z_{j-1}}{2}\right)Y_j\left(\frac{1+Z_{j+1}}{2}\right) - \left(\frac{1-Z_{j-1}}{2}\right)Y_j\left(\frac{1-Z_{j+1}}{2}\right)\right\}, \quad (6)$$

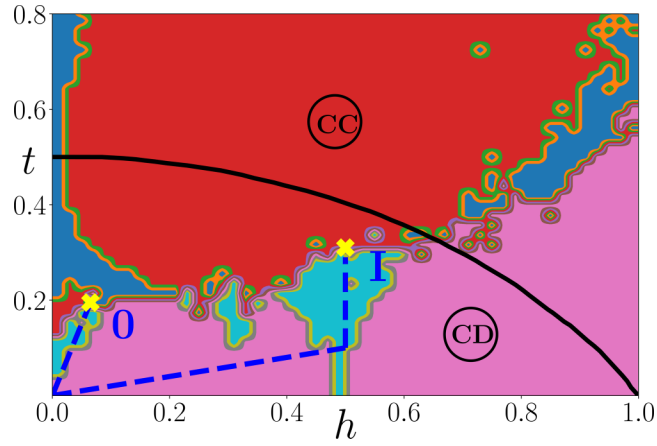


FIG. 1. Properties of the Ising model (5) in $t - h$ parameter space for $L = 16$ and $\mu = 1$. QMBSs may exist in chaotic regions with a mean gap ratio $r > 0.5$ and low-entanglement entropy $S < 0.5$ with respect to the GOE value. The corresponding disconnected blue region lies entirely in the charge deconfined (CD) regime. The charge confinement (CC) region lies mainly within the regime of chaotic, $r > 0.5$, but with lowest entropy states, $S > 0.5$, thus with no chance for QMBSs. The pink color marks the mixed dynamics regime, $r < 0.5$, $S < 0.5$; in the dark blue region, $r < 0.5$, $S > 0.5$. "0" and "I" denote paths along which QMBS states are followed using level dynamics.

to obtain an effective Hamiltonian $H_{\text{eff}} = e^S H e^{-S} = H + [S, H] + \mathcal{O}(t^2)$. Notice that S is chosen in such a way that the new terms commute with the unperturbed part of the Hamiltonian $\sum_{i=1}^{L}\frac{\mu}{2}Z_iZ_{i+1}$ to the leading order in the expansion, thus preserving its block-diagonal structure while also including all virtual processes within each sector. The derived effective Hamiltonian,

$$H_{\text{eff}} = \sum_{i=1}^{L}\frac{\mu}{2}Z_iZ_{i+1} - hZ_i - \frac{t}{2}(X_i - Z_{i-1}X_iZ_{i+1}), \quad (7)$$

turns out to be the well-known model discussed in detail in Ref. [13], where two towers of QMBSs have been identified. The latter are of the form

$$|S_n^k\rangle = \frac{1}{n!\sqrt{\mathcal{N}(L,n)}}[(\mathcal{Q}^k)^\dagger]^n|\Omega^k\rangle, \quad (8)$$

with $k = 1, 2$, $|\Omega^1\rangle = |0\cdots0\rangle$, $|\Omega^2\rangle = |1\cdots1\rangle$, and $(\mathcal{Q}^k)^\dagger = \sum_{i=i_1}^{i_L}(-1)^i P^k_{i-1}[X_i + (-1)^k Y_i]P^k_{i+1}$, with projection operators $P_i^k = [1 + (-1)^k Z_i]/2$. Such QBMSs describe n-magnon and n-antimagnons excitations for $k = 1$ and $k = 2$, respectively [13].

As already pointed out, the Schrieffer-Wolff transformation described above links the models (5) and (1) with the effective spin model (7) only for $t \ll \mu$. In this limit, the states given by Eq. (8) become true QMBSs of Hamiltonian (7), as it was studied in Ref. [13]. It appears natural to wonder whether, following the states (8) in the parameter space, it is possible to also find scarred states in the gauged Kitaev chain beyond the $t \ll \mu$ limit.

Level dynamics. In order to investigate this point, we first determine in which regime of parameters the model (5) can be considered as ergodic, and thus where the regular states may

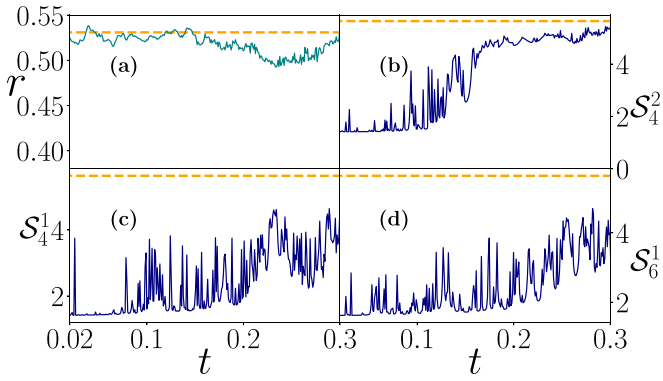


FIG. 2. (a) The gap ratio r and (b) half-chain entanglement entropy ($\mathcal{S}$) along path 0 for the S_4^2 state from the antimagnon family; (c) S_4^1 and (d) S_6^1 from the magnon family, all for $L = 18$. States may be followed despite narrow avoided crossings indicated by spikes of the entanglement entropy. The antimagnon state loses its low EE feature around $t = 0.14$ while magnonlike QMBSs may be followed up to $t \approx 0.2$.

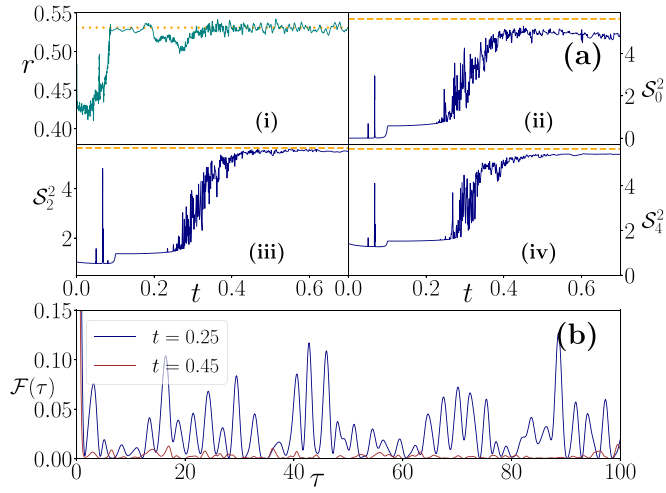


FIG. 3. (a) is as Fig. 2 but for path I and $L = 18$. Along this path only antimagnon excitations may be followed while magnons appear at the edges of the energy spectrum only. (b) Time dependence of the fidelity relative to an initial state $|\psi(0)\rangle$ and evolved with (5) at $h = 0.5$ and different values of t for $L = 16$ ($\mu = 1$).

be called QMBSs. Ergodicity may be revealed by the adjacent mean gap ratio r [65] between subsequent level spacings Δ_i,

$$r_i = \frac{\min\{\Delta_i, \Delta_{i+1}\}}{\max\{\Delta_i, \Delta_{i+1}\}}, \tag{9}$$

where $r \simeq 0.531$ corresponds to the fully ergodic regime [as described by the Gaussian orthogonal ensemble (GOE) [66]] and $r \simeq 0.386$ indicates the quasi-integrable regime [65,67]. As shown in Fig. 1, our model shows strong indications of near-integrable behavior for $h \ll \mu$ or $t \ll \mu$. Outside this region, the model is expected to be nonintegrable. The next step is then to identify the region where the entanglement entropy (EE) of some eigenstates is well below the GOE estimate, as QMBSs should have low, subvolume entropy. The half-chain EE is defined in a standard way as $\mathcal{S} = -\mathrm{Tr}[\rho_{L/2} \ln \rho_{L/2}]$ [68]. We compare it to the typical GOE value for a given system size. Once the two lowest EE states have a relative EE sufficiently low (say half of the GOE value), there is the chance that those states are indeed scarred. Figure 1 shows by a light blue color the domains where both $r > 0.5$ and states with a sufficiently low EE exist.

With the suspected regions identified, we start the analysis with $|S_n^k\rangle$ states for the Hamiltonian (5) with parameters $t, h \ll \mu$, e.g., for $t_0 = h_0 = 0.001$ (we set $\mu = 1$ in the following), with the aim of tracking such initial states $|S_n^k(t_0, h_0)\rangle$ following their possible deformations induced by making small changes in the parameters, $t = t_0 + \delta t$ and $h = h_0 + \delta h$. As examples we consider paths indicated by "0" and "I" in Fig. 1.

Every time we update the parameters, we diagonalize the Hamiltonian in the symmetry sector with momentum $p = 0$ and parity $+1$ (we consider n even only) and find the new candidate $|E_n(t, h)\rangle$ by maximizing the overlap $O = |\langle E_n(t, h)|S_n^k\rangle|$. For an isolated level, the new state is accepted, $|S_n^k\rangle$ is updated, and we repeat the procedure. Special care is taken to diabatically cross narrow avoided crossings [68].

Figure 2 shows tracking the QMBS states identified as $|S_n^k(t, h)\rangle$ along path 0. Both magnon and antimagnon excitations, as given by (8), may be followed. This path lies almost fully in the chaotic regime as revealed by r statistics, so the observed low EE states may be truly considered as QMBSs, observed, let us stress, deep in the deconfined region.

The path indicated as I also remains in the deconfined phase, extending to large values of h (cf. Fig. 1). Levels are followed through a regular, weakly perturbed region, along the straight line $t = 0.2h$ up to $h = 0.5$. Then path I turns upwards, staying in the chaotic region up to the point $(t, h) = (0.3, 0.5)$. Along this vertical part, the tracked low EE states, shown in Fig. 3(a), are truly the QMBSs embedded in the chaotic spectrum. As seen from the EE values, the scarred character of the followed states is slowly lost due to, as verified [68], various avoided crossings.

As discussed in the Introduction, the presence of QMBSs can be further revealed by the persistent time oscillations of an out-of-equilibrium configuration. To reveal this aspect, we prepare an initial state given by the equal superposition of two states of the form (8) for small t, h values, $|\psi(0)\rangle = \frac{1}{\sqrt{2}}(|S_0^2\rangle + |S_2^2\rangle)$. After this initialization, we let this state evolve with Hamiltonian (5) and we calculate the fidelity $\mathcal{F}(\tau) = |\langle\psi(0)|\psi(\tau)\rangle|^2$, where τ is the time (in units of inverse μ). At $t = 0.25$, we observe for other choices of finite persistent oscillations of $\mathcal{F}(\tau)$ as expected for QMBS states, and this behavior persists until the end of path I [compare Fig. 3(b)]. Beyond this limit ($t > 0.3$), low-entanglement states disappear and $\mathcal{F}(\tau)$ shows irregular oscillations around the mean value of about $1/L^2$, as expected for thermal states.

Figure 4 visualizes the presence of QMBSs by showing the value of $\mathcal{S}$ for all eigenstates at $t = 0.2$ and $h = 0.5$, where the system is in the weak ergodic regime. The entropy still reveals a fingerlike structure that indicates the existence of hidden, unidentified symmetries. The states enclosed in circles are those tracked up from the near-integrable limit. The

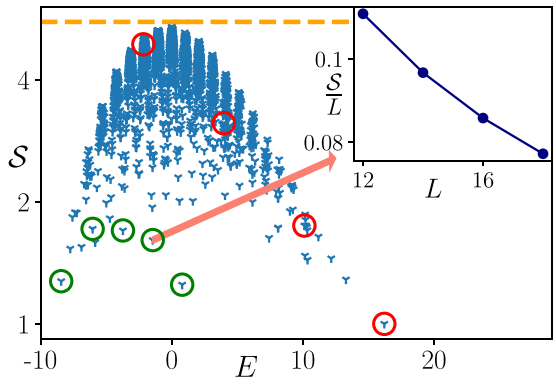


FIG. 4. The half-chain entanglement entropy ($\mathcal{S}$) of all the eigenstates at $t = 0.2$, $h = 0.5$ for $L = 16$. The orange dashed line gives the $\mathcal{S}_{\mathrm{RMT}}$ value. Circles denote different QMBSs obtained via our tracking procedure. Green circles denote the antimagnonlike family S_n^2 for $n = 0, 2, 4, 6, 8$ while red circles the magnonlike states S_n^1 with $n = 0, \ldots, 6$ counting from the right-hand side. Inset: The half-chain entanglement entropy divided by system size ($\frac{\mathcal{S}}{L}$) for the S_2^2 state showing its subvolume property as expected for QMBSs.

members of the antimagnonlike family S_k^2, denoted by green circles, have very low-entanglement entropies as compared to other states of similar energy. They are thus truly QMBSs. The inset reveals a subvolume scaling of the entanglement entropy of the S_2^2 state. The magnon excitations, on the other hand, dissolve among other states (in the high density of states region).

In summary, motivated by recent predictions of finding QMBS states in a confined regime [59,69] of LGTs, we investigated the thermalization properties of the gauged Kitaev chain. We observe that deep in the confined phase even states with the smallest entanglement entropy have relatively large, volume-law values indicating a lack of QMBSs. On the other hand, for relatively large values of the electric field, some states reveal low-entanglement entropy. We can identify these states by following them from the very small t, h values for which analytic predictions are available [13]. Such states result to be true QMBSs and are found uniquely in the deconfined phase, which turns out to be a weakly ergodic regime characterized by the GOE-like mean gap ratio. The presence of QMBSs has been further verified by studying their time dynamics. By building an initial state given by the superposition of two QMBSs, the fidelity of the state shows pronounced oscillations with no sign of thermalization. The adiabatic following of the states breaks down at the end points of our chosen paths due to energy-level mixing, where interestingly QMBSs also disappear. In conclusion, our results unambiguously reveal that QMBSs occur even in deconfined regimes of LGTs, thus paving the way toward a deeper understanding of the connection between the lack of thermalization and local symmetries.

Acknowledgments. We thank A. Bohrdt, U. Borla, F. Grusdt, J. C. Halimeh, P. Hauke, M. Kebric, S. Moroz, and P. Sierant for discussions on this manuscript and related projects. The numerical computations have been possible owing to PL-Grid Infrastructure. The works of A.S.A. and J.Z. have been realized within the Opus Grant No. 2019/35/B/ST2/00034, financed by National Science Centre (Poland). ICFO group acknowledges support from ERC AdG NOQIA; Agencia Estatal de Investigación (R&D project CEX2019-000910-S, funded by MCIN/AEI/10.13039/501100011033, Plan National FIDEUA PID2019-106901GB-I00, FPI, QUANTERA MAQS PCI2019-111828-2/10.13039/501100011033), QUANTERA DYNAMITE PCI2022-132919, Proyectos de I+D+I "Retos Colaboración" QUSPIN RTC2019-007196-7), MCIN via European Union NextGenerationEU (PRTR); Fundació Privada Cellex; Fundació Mir-Puig; Generalitat de Catalunya through the European Social Fund FEDER and CERCA program (AGAUR Grant No. 2017 SGR 1341, QuantumCAT \ U16-011424, co-funded by ERDF Operational Program of Catalonia 2014-2020); EU Horizon 2020 FET-OPEN OPTOlogic (Grant No 899794); National Science Centre, Poland (Symfonia Grant No. 2016/20/W/ST4/00314); European Union's Horizon 2020 research and innovation programme under the Marie-Skodowska-Curie grant agreement No 101029393 (STREDCH) and No 847648 ("La Caixa" Junior Leaders fellowships ID100010434 LCF/BQ/PI19/11690013, LCF/BQ/PI20/11760031, LCF/BQ/PR20/11770012, LCF/BQ/PR21/11840013). D.G.-C. is supported by the Simons Collaboration on Ultra-Quantum Matter, which is a grant from the Simons Foundation (651440, P.Z.).

[1] M. Rigol, V. Dunjko, and M. Olshanii, Thermalization and its mechanism for generic isolated quantum systems, Nature (London) **452**, 854 (2008).

[2] A. Polkovnikov, K. Sengupta, A. Silva, and M. Vengalattore, Colloquium: Nonequilibrium dynamics of closed interacting quantum systems, Rev. Mod. Phys. **83**, 863 (2011).

[3] C. Gogolin and J. Eisert, Equilibration, thermalization, and the emergence of statistical mechanics in closed quantum systems, Rep. Prog. Phys. **79**, 056001 (2016).

[4] L. Vidmar and M. Rigol, Generalized Gibbs ensemble in integrable lattice models, J. Stat. Mech.: Theory Exp. (2016) 064007.

[5] H. Bernien, S. Schwartz, A. Keesling, H. Levine, A. Omran, H. Pichler, S. Choi, A. S. Zibrov, M. Endres, M. Greiner, V. Vuletić, and M. D. Lukin, Probing many-body dynamics on a 51-atom quantum simulator, Nature (London) **551**, 579 (2017).

[6] N. Shiraishi and T. Mori, Systematic Construction of Counterexamples to the Eigenstate Thermalization Hypothesis, Phys. Rev. Lett. **119**, 030601 (2017).

[7] C. J. Turner, A. A. Michailidis, D. A. Abanin, M. Serbyn, and Z. Papić, Weak ergodicity breaking from quantum many-body scars, Nat. Phys. **14**, 745 (2018).

[8] C. J. Turner, A. A. Michailidis, D. A. Abanin, M. Serbyn, and Z. Papić, Quantum scarred eigenstates in a Rydberg atom chain:

Entanglement, breakdown of thermalization, and stability to perturbations, Phys. Rev. B **98**, 155134 (2018).

[9] S. Moudgalya, S. Rachel, B. A. Bernevig, and N. Regnault, Exact excited states of nonintegrable models, Phys. Rev. B **98**, 235155 (2018).

[10] S. Moudgalya, N. Regnault, and B. A. Bernevig, Entanglement of exact excited states of Affleck-Kennedy-Lieb-Tasaki models: Exact results, many-body scars, and violation of the strong eigenstate thermalization hypothesis, Phys. Rev. B **98**, 235156 (2018).

[11] T. Iadecola and M. Žnidarič, Exact Localized and Ballistic Eigenstates in Disordered Chaotic Spin Ladders and the Fermi-Hubbard Model, Phys. Rev. Lett. **123**, 036403 (2019).

[12] M. Schecter and T. Iadecola, Weak Ergodicity Breaking and Quantum Many-Body Scars in Spin-1 XY Magnets, Phys. Rev. Lett. **123**, 147201 (2019).

[13] T. Iadecola and M. Schecter, Quantum many-body scar states with emergent kinetic constraints and finite-entanglement revivals, Phys. Rev. B **101**, 024306 (2020).

[14] M. Serbyn, D. A. Abanin, and Z. Papić, Quantum many-body scars and weak breaking of ergodicity, Nat. Phys. **17**, 675 (2021).

[15] K. Lee, R. Melendrez, A. Pal, and H. J. Changlani, Exact three-colored quantum scars from geometric frustration, Phys. Rev. B **101**, 241111(R) (2020).

[16] F. M. Surace, P. P. Mazza, G. Giudici, A. Lerose, A. Gambassi, and M. Dalmonte, Lattice Gauge Theories and String Dynamics in Rydberg Atom Quantum Simulators, Phys. Rev. X **10**, 021041 (2020).

[17] G. Magnifico, M. Dalmonte, P. Facchi, S. Pascazio, F. V. Pepe, and E. Ercolessi, Real time dynamics and confinement in the $\mathbb{Z}_n$ Schwinger-Weyl lattice model for 1+1 QED, Quantum **4**, 281 (2020).

[18] T. Chanda, J. Zakrzewski, M. Lewenstein, and L. Tagliacozzo, Confinement and Lack of Thermalization after Quenches in the Bosonic Schwinger Model, Phys. Rev. Lett. **124**, 180602 (2020).

[19] H. Zhao, J. Vovrosh, F. Mintert, and J. Knolle, Quantum Many-Body Scars in Optical Lattices, Phys. Rev. Lett. **124**, 160604 (2020).

[20] Z. Papić, Weak ergodicity breaking through the lens of quantum entanglement, arXiv:2108.03460.

[21] S. Moudgalya, A. Prem, R. Nandkishore, N. Regnault, and B. A. Bernevig, Thermalization and its absence within Krylov subspaces of a constrained Hamiltonian, in *Memorial Volume for Shoucheng Zhang*, edited by B. Lian, C. X. Liu, E. Demler, S. Kivelson, and X. Qi (World Scientific, Singapore, 2021), p. 147.

[22] F. M. Surace, M. Dalmonte, and A. Silva, Quantum local random networks and the statistical robustness of quantum scars, arXiv:2107.00884.

[23] H. Zhao, A. Smith, F. Mintert, and J. Knolle, Orthogonal Quantum Many-Body Scars, Phys. Rev. Lett. **127**, 150601 (2021).

[24] T. Szołdra, P. Sierant, M. Lewenstein, and J. Zakrzewski, Unsupervised detection of decoupled subspaces: Many-body scars and beyond, arXiv:2201.07151.

[25] D. Bluvstein, A. Omran, H. Levine, A. Keesling, G. Semeghini, S. Ebadi, T. T. Wang, A. A. Michailidis, N. Maskara, W. W. Ho, S. Choi, M. Serbyn, M. Greiner, V. Vuletić, and M. D. Lukin, Controlling quantum many-body dynamics in driven Rydberg atom arrays, Science **371**, 1355 (2021).

[26] C. J. Turner, J.-Y. Desaules, K. Bull, and Z. Papić, Correspondence Principle for Many-Body Scars in Ultracold Rydberg Atoms, Phys. Rev. X **11**, 021021 (2021).

[27] E. J. Heller, Bound-State Eigenfunctions of Classically Chaotic Hamiltonian Systems: Scars of Periodic Orbits, Phys. Rev. Lett. **53**, 1515 (1984).

[28] M. C. Gutzwiller, Periodic orbits and classical quantization conditions, J. Math. Phys. **12**, 343 (1971).

[29] E. Bogomolny, Smoothed wavefunctions of chaotic quantum systems, Physica D **31**, 169 (1988).

[30] D. Delande and J. C. Gay, Scars of symmetries in quantum chaos, Phys. Rev. Lett. **59**, 1809 (1987).

[31] D. Jaksch and P. Zoller, The cold atom Hubbard toolbox, Ann. Phys. **315**, 52 (2005).

[32] M. Lewenstein, A. Sanpera, V. Ahufinger, B. Damski, A. Sen(De), and U. Sen, Ultracold atomic gases in optical lattices: Mimicking condensed matter physics and beyond, Adv. Phys. **56**, 243 (2007).

[33] C. Gross and I. Bloch, Quantum simulations with ultracold atoms in optical lattices, Science **357**, 995 (2017).

[34] F. Schäfer, T. Fukuhara, S. Sugawa, Y. Takasu, and Y. Takahashi, Tools for quantum simulation with ultracold atoms in optical lattices, Nat. Rev. Phys. **2**, 411 (2020).

[35] A. Browaeys and T. Lahaye, Many-body physics with individually controlled Rydberg atoms, Nat. Phys. **16**, 132 (2020).

[36] G.-X. Su, H. Sun, A. Hudomal, J.-Y. Desaules, Z.-Y. Zhou, B. Yang, J. C. Halimeh, Z.-S. Yuan, Z. Papić, and J.-W. Pan, Observation of unconventional many-body scarring in a quantum simulator, arXiv:2201.00821.

[37] E. A. Martinez, C. A. Muschik, P. Schindler, D. Nigg, A. Erhard, M. Heyl, P. Hauke, M. Dalmonte, T. Monz, P. Zoller, and R. Blatt, Real-time dynamics of lattice gauge theories with a few-qubit quantum computer, Nature (London) **534**, 516 (2016).

[38] C. Schweizer, F. Grusdt, M. Berngruber, L. Barbiero, E. Demler, N. Goldman, I. Bloch, and M. Aidelsburger, Floquet approach to $\mathbb{Z}_2$ lattice gauge theories with ultracold atoms in optical lattices, Nat. Phys. **15**, 1168 (2019).

[39] F. Görg, K. Sandholzer, J. Minguzzi, R. Desbuquois, M. Messer, and T. Esslinger, Realization of density-dependent Peierls phases to engineer quantized gauge fields coupled to ultracold matter, Nat. Phys. **15**, 1161 (2019).

[40] A. Mil *et al.*, A scalable realization of local U(1) gauge invariance in cold atomic mixtures, Science **367**, 1128 (2020).

[41] Z.-C. Yang, F. Liu, A. V. Gorshkov, and T. Iadecola, Hilbert-Space Fragmentation from Strict Confinement, Phys. Rev. Lett. **124**, 207602 (2020).

[42] B. Yang, H. Sun, R. Ott, H. Y. Wang, T. V. Zache, J. C. Halimeh, Z. S. Yuan, P. Hauke, and J. W. Pan, Observation of gauge invariance in a 71-site Bose-Hubbard quantum simulator, Nature (London) **587**, 392 (2020).

[43] E. Zohar and B. Reznik, Confinement and Lattice Quantum-Electrodynamic Electric Flux Tubes Simulated with Ultracold Atoms, Phys. Rev. Lett. **107**, 275301 (2011).

[44] M. Dalmonte and S. Montangero, Lattice gauge theory simulations in the quantum information era, Contemp. Phys. **57**, 388 (2016).

[45] F. F. Assaad and T. Grover, Simple Fermionic Model of Deconfined Phases and Phase Transitions, Phys. Rev. X **6**, 041049 (2016).

[46] D. González-Cuadra, E. Zohar, and J. I. Cirac, Quantum simulation of the Abelian-Higgs lattice gauge theory with ultracold atoms, New J. Phys. **19**, 063038 (2017).

[47] S. Gazit, M. Randeria, and A. Vishwanath, Emergent Dirac fermions and broken symmetries in confined and deconfined phases of Z_2 gauge theories, Nat. Phys. **13**, 484 (2017).

[48] S. Gazit, F. F. Assaad, S. Sachdev, A. Vishwanath, and C. Wang, Confinement transition of $\mathbb{Z}_2$ gauge theories coupled to massless fermions: Emergent quantum chromodynamics and SO(5) symmetry, Proc. Natl. Acad. Sci. USA **115**, E6987 (2018).

[49] L. Barbiero, C. Schweizer, M. Aidelsburger, E. Demler, N. Goldman, and F. Grusdt, Coupling ultracold matter to dynamical gauge fields in optical lattices: From flux attachment to $\mathbb{Z}_2$ lattice gauge theories, Sci. Adv. **5**, eaav7444(2019).

[50] U. Borla, R. Verresen, F. Grusdt, and S. Moroz, Confined Phases of One-Dimensional Spinless Fermions Coupled to Z_2 Gauge Theory, Phys. Rev. Lett. **124**, 120503 (2020).

[51] D. González-Cuadra, L. Tagliacozzo, M. Lewenstein, and A. Bermudez, Robust Topological Order in Fermionic $\mathbb{Z}_2$ Gauge Theories: From Aharonov-Bohm Instability to Soliton-Induced Deconfinement, Phys. Rev. X **10**, 041007 (2020).

[52] M. C. Bañuls, R. Blatt, J. Catani, A. Celi, J. I. Cirac, M. Dalmonte, L. Fallani, K. Jansen, M. Lewenstein, S. Montangero, C. A. Muschik, B. Reznik, E. Rico, L. Tagliacozzo, K. Van Acoleyen, F. Verstraete, U.-J. Wiese, M. Wingate, J. Zakrzewski, and P. Zoller, Simulating lattice gauge theories within quantum technologies, Eur. Phys. J. D **74**, 165 (2020).

[53] J. C. Halimeh and P. Hauke, Reliability of Lattice Gauge Theories, Phys. Rev. Lett. **125**, 030503 (2020).

[54] J. C. Halimeh, L. Homeier, C. Schweizer, M. Aidelsburger, P. Hauke, and F. Grusdt, Stabilizing lattice gauge theories through simplified local pseudo generators, arXiv:2108.02203.

[55] M. V. Damme, J. Mildenberger, F. Grusdt, P. Hauke, and J. C. Halimeh, Suppressing nonperturbative gauge errors in the thermodynamic limit using local pseudogenerators, arXiv:2110.08041.

[56] M. Kebrič, L. Barbiero, C. Reinmoser, U. Schollwöck, and F. Grusdt, Confinement and Mott Transitions of Dynamical Charges in One-Dimensional Lattice Gauge Theories, Phys. Rev. Lett. **127**, 167203 (2021).

[57] M. Aidelsburger, L. Barbiero, A. Bermudez, T. Chanda, A. Dauphin, D. González-Cuadra, P. R. Grzybowski, S. Hands, F. Jendrzejewski, J. Jünemann, G. Juzeliūnas, V. Kasper, A. Piga, S.-J. Ran, M. Rizzi, G. Sierra, L. Tagliacozzo, E. Tirrito, T. V. Zache, J. Zakrzewski *et al.*, Cold atoms meet lattice gauge theory, Philos. Trans. R. Soc. A **380**, 20210064 (2022).

[58] D. Banerjee and A. Sen, Quantum Scars from Zero Modes in an Abelian Lattice Gauge Theory on Ladders, Phys. Rev. Lett. **126**, 220601 (2021).

[59] I.-C. Chen and T. Iadecola, Emergent symmetries and slow quantum dynamics in a Rydberg-atom chain with confinement, Phys. Rev. B **103**, 214304 (2021).

[60] A. Lerose, F. M. Surace, P. P. Mazza, G. Perfetto, M. Collura, and A. Gambassi, Quasilocalized dynamics from confinement of quantum excitations, Phys. Rev. B **102**, 041118(R) (2020).

[61] U. Borla, R. Verresen, J. Shah, and S. Moroz, Gauging the Kitaev chain, SciPost Phys. **10**, 148 (2021).

[62] J. B. Kogut, An introduction to lattice gauge theory and spin systems, Rev. Mod. Phys. **51**, 659 (1979).

[63] A. A. Ovchinnikov, D. V. Dmitriev, V. Y. Krivnov, and V. O. Cheranovskii, Antiferromagnetic ising chain in a mixed transverse and longitudinal magnetic field, Phys. Rev. B **68**, 214406 (2003).

[64] A. Bastianello, U. Borla, and S. Moroz, Fragmentation and Emergent Integrable Transport in the Weakly Tilted Ising Chain, Phys. Rev. Lett. **128**, 196601 (2022).

[65] V. Oganesyan and D. A. Huse, Localization of interacting fermions at high temperature, Phys. Rev. B **75**, 155111 (2007).

[66] F. Haake, *Quantum Signatures of Chaos* (Springer, Berlin, 2010).

[67] Y. Y. Atas, E. Bogomolny, O. Giraud, and G. Roux, Distribution of the Ratio of Consecutive Level Spacings in Random Matrix Ensembles, Phys. Rev. Lett. **110**, 084101 (2013).

[68] See Supplemental Material at http://link.aps.org/supplemental/10.1103/PhysRevB.106.L041101 for details on entanglement entropy, the state following analysis, and the fate of magnons, which includes Refs. [27,30,70–75].

[69] A. J. A. James, R. M. Konik, and N. J. Robinson, Nonthermal States Arising from Confinement in One and Two Dimensions, Phys. Rev. Lett. **122**, 130603 (2019).

[70] L. Vidmar and M. Rigol, Entanglement Entropy of Eigenstates of Quantum Chaotic Hamiltonians, Phys. Rev. Lett. **119**, 220603 (2017).

[71] Y. Huang, Universal eigenstate entanglement of chaotic local Hamiltonians, Nucl. Phys. B **938**, 594 (2019).

[72] Y. Huang, Universal entanglement of mid-spectrum eigenstates of chaotic local Hamiltonians, Nucl. Phys. B **966**, 115373 (2021).

[73] H. Stöckmann, *Quantum Chaos: An Introduction* (Cambridge University Press, Cambridge, U.K., 1999).

[74] J. Zakrzewski and M. Kuś, Distributions of avoided crossings for quantum chaotic systems, Phys. Rev. Lett. **67**, 2749 (1991).

[75] J. Zakrzewski, D. Delande, and M. Kuś, Parametric motion of energy levels in quantum chaotic systems. II. Avoided-crossing distributions, Phys. Rev. E **47**, 1665 (1993).